Contribution from the Laboratory for Electron Spectroscopy and Surface Analysis, Department of Chemistry, University of Arizona, Tucson, Arizona 85721, Arthur Amos Noyes Laboratory,[⊥] California Institute of Technology, Pasadena, California 91125, and Department of Chemistry, University of Pittsburgh, Pittsburgh, Pennsylvania 15260

Valence Electronic Structure of Bis(pyrazolyl)-Bridged Iridium Dicarbonyl Dimers. Electronic Effects of 3,5-Dimethylpyrazolyl Substitution on Metal-Metal Interactions

Dennis L. Lichtenberger,*[,†] Ann S. Copenhaver,[†] Harry B. Gray,*[,‡] Janet L. Marshall,[‡,§] and Michael D. Hopkins[∥]

Received March 31, 1988

The He I valence photoelectron spectra of $[Ir(\mu\text{-pyrazolyl})(CO)_2]_2$, $[Ir(\mu\text{-3-methylpyrazolyl})(CO)_2]_2$, and $[Ir(\mu\text{-3,5-dimethylpyrazolyl})(CO)_2]_2$ have been obtained. These complexes may be viewed as two square-planar d^8 iridium centers held together by two bridging pyrazolyl ligands to form a six-membered Ir-$(N-N)_2$-Ir ring. The ring is in a boat conformation with the iridium atoms positioned at the bow and stern such that interaction is possible between the filled d_{z^2} orbitals from each metal center. The 3,5-dimethylpyrazolyl complex is active as a hydrogenation catalyst while the other related complexes are not. It has been proposed previously that greater filled-filled orbital interaction between the metal centers in the dimethyl complex (as caused by the shorter metal-metal distance) accounts for the greater reactivity. It is found here that there is indeed substantial interaction between the d_{z^2} atomic orbitals of the two iridium centers, and the ionization corresponding to the Ir-Ir antibonding d_{z^2}-d_{z^2} interaction is the lowest energy ionization band of these complexes. This ionization is cleanly separated from the other ionizations of the complexes. Of particular interest is the broad and unusual asymmetry found in the band profile of the initial ionization, which indicates appreciable vibrational excitation associated with the shortening of the metal-metal distance upon removal of an electron from this molecular orbital. The energy of the first ionization band is very sensitive to the methyl substitutions on the pyrazolyl groups. The sensitivity of this ionization to methyl substitution (and in turn the change in reaction chemistry between these complexes) is due more to the electronic inductive effects of the methyl group substitutions than to changes in geometry and splitting of the bonding and antibonding combinations of the metal d_{z^2} orbitals.

Introduction

Pyrazolyl-bridged iridium dimers have shown potential in hydrogenation catalysis, photochemistry, and redox chemistry.[1-4] The reactivity of these metal dimer systems has been related to the geometry maintained by the d^8 metal center, as shown in Figure 1. The local geometry at each iridium center is the familiar d^8 square-planar arrangement with cis carbonyls, and the two square planes of the iridium centers are held together via the pyrazolyl bridges. This arrangement allows for the formation of a six-membered Ir-$(N-N)_2$-Ir ring in the boat conformation with the metals at the bow and the stern positions. As the pyrazolyl bridges draw the metals together, the interaction between the filled metal d_{z^2} levels of the d^8 configurations increases. It has been suggested that appropriately small metal-metal distances can lead to appreciable destabilization of the antibonding combination of the filled-filled interaction and promote reactions of the complex.[1,2] $[Ir(\mu\text{-3,5-Me}_2\text{-pz})(CO)_2]_2$ (where 3,5-Me_2-pz = 3,5-dimethylpyrazolyl) has shown catalytic activity in hydrogenation reactions. It possesses a shorter metal-metal distance (3.245 Å) than the related compounds $[Ir(\mu\text{-3-Me-pz})(CO)_2]_2$ (where 3-Me-pz = 3-methylpyrazolyl) and $[Ir(\mu\text{-pz})(CO)_2]_2$ (3.502 Å) (where pz = pyrazolyl), which do not exhibit catalytic activity.[1]

Photoelectron spectroscopy can provide a direct experimental measure of the electronic interactions in these metal-metal complexes.[5,6] The technique has often been used to study through-space lone-pair (filled-filled) interactions such as those that occur in nitrogen-, oxygen-, or sulfur-containing molecules.[7,8] The photoelectron spectra presented in this paper show the magnitude of the through-space filled-filled interaction between the metal centers. It is found that this interaction is significant in providing a low-energy, metal-localized ionization that is separated from the other ionizations of the complex. However, the trends in oxidation and reaction behavior with methyl substitution are found to be more dependent on inductive electronic effects than on changes in the filled-filled interaction and geometry of the complex.

Experimental Section

Photoelectron Spectra. The photoelectron spectra were measured on a spectrometer with specially designed photon sources, ionization cells, 36 cm radius hemispherical analyzer (McPherson), power supplies, counter interface, and collection methods that have been described elsewhere.[9-13] The spectra were measured with the sample ionization cell at 80-85 °C. The argon ionization at 15.759 eV was used as an internal calibration lock of the energy scale (±0.003 eV). The data are represented analytically in terms of asymmetric Gaussian peaks, which are defined by parameters representing the position of the peak, the half-widths on the high (W_h) and low (W_l) binding energy sides of the peak, and the amplitude of the peak as determined by the program GFIT.[14]

Calculations. Molecular orbital calculations were performed by using the Fenske-Hall method.[15] Iridium functions for the calculations were generated by the Method of Bursten, Jensen, and Fenske.[16] In order to judge the sensitivity of the results to the diffuseness of the metal basis functions, the calculations were performed with iridium functions from atomic oxidation states of 0, +1, and +2. Ir(I) functions were found to be consistent with the calculated d-orbital occupation and were used for the calculations shown. The iridium functions were single-ζ functions for all the core atomic orbitals and double-ζ for the 5d orbitals. The 6s and 6p orbitals were represented by single-ζ functions with an exponent of 2.0. The N, C, and O atoms had double-ζ 2p functions while hydrogen

* To whom correspondence should be addressed.
† University of Arizona.
‡ California Institute of Technology.
§ Present address: Miami Valley Laboratories, The Procter and Gamble Co., P.O. Box 39175, Cincinnati, OH 45247.
∥ University of Pittsburgh.
⊥ Contribution No. 7755.

(1) Nussbaum, S.; Rettig, S. J.; Storr, A.; Trotter, J. *Can. J. Chem.* **1985**, *63*, 692.
(2) Beveridge, K. A.; Bushnell, G. W.; Stobart, S. R.; Atwood, J. L.; Zaworotho, M. J. *Organometallics* **1983**, *2*, 1447.
(3) (a) Beveridge, K. A.; Bushnell, G. W.; Dixon, K. R.; Eadie, D. T.; Stobart, S. R.; Atwood, J. L.; Zaworotho, M. J. *J. Am. Chem. Soc.* **1982**, *104*, 920. (b) Coleman, A. W.; Eadie, D. T.; Stobart, S. R. *J. Am. Chem. Soc.* **1982**, *104*, 922.
(4) (a) Fox, L. S.; Marshall, J. L.; Gray, H. B.; Winkler, J. R. *J. Am. Chem. Soc.* **1987**, *109*, 690. (b) Marshall, J. L.; Stiegman, A. E.; Gray, H. B. *ACS Symp. Ser.* **1986**, *No. 307*, 166.
(5) Cotton, F. A.; Walton, R. A. *Multiple Bonds Between Metal Atoms*; Wiley: New York, 1982.
(6) Van Dam, H.; Osdam, A. *Transition Met. Chem. (London)* **1985**, *9*, 125.
(7) Sweigart, D. A.; Turner, D. W. *J. Am. Chem. Soc.* **1972**, *94*, 5599.
(8) Heilbronner, E.; Muszkat, K. A. *J. Am. Chem. Soc.* **1970**, *92*, 3818.
(9) Calabro, D. C.; Hubbard, J. L.; Blevins, C. H., II; Campbell, A. C.; Lichtenberger, D. L. *J. Am. Chem. Soc.* **1981**, *103*, 6739.
(10) Lichtenberger, D. L.; Calabro, D. C.; Kellogg, G. E. *Organometallics* **1984**, *3*, 1623.
(11) Hubbard, J. L. *Diss. Abstr. Int., B* **1983**, *43*, 2203.
(12) Kellogg, G. E. *Diss. Abstr. Int., B* **1986**, *46*, 3838.
(13) Lichtenberger, D. L.; Kellogg, G. E.; Kristofzski, J. G.; Page, D.; Turner, S.; Klinger, G.; Lorenzen, J. *Rev. Sci. Instrum.* **1986**, *57*, 2366.
(14) Lichtenberger, D. L.; Fenske, R. F. *J. Am. Chem. Soc.* **1976**, *98*, 50.
(15) Hall, M. B.; Fenske, R. F. *Inorg. Chem.* **1972**, *11*, 768.
(16) Bursten, B. E.; Jensen, J. R.; Fenske, R. F. *J. Chem. Phys.* **1978**, *68*, 3320.

0020-1669/88/1327-4488$01.50/0

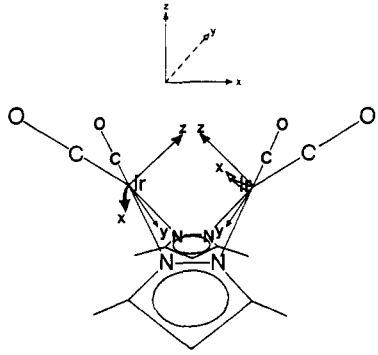

Figure 1. Basic geometry of the iridium dimer complexes and the coordinate system for calculations and discussion of the electronic structure.

possessed a single-ζ function with an exponent of 1.2.

The bond distances and angles were taken from crystal structures of $[Ir(\mu\text{-pz})(CO)_2]_2$ and $[Ir(\mu\text{-3,5-Me}_2\text{-pz})(CO)_2]_2$[1] with carbon–hydrogen distances taken to be 1.1 Å. The coordinate system for the calculations is shown in Figure 1. The coordinate system about each metal was oriented so that the z axis of the metal is normal to the square plane of coordinated ligands and the x and y axes bisect the coordinated ligands found about each metal. Each geometry was idealized to C_{2v} symmetry.

Calculations were also performed by using Rh(I) functions[17] to further test the sensitivity of the calculations to the basis functions and to relate the results of the present study to similar rhodium complexes. We observed little difference between the calculated trends and molecular orbital ordering of iridium versus those of rhodium. However, the predominantly metal iridium σ^* molecular orbital energy tended to be destabilized on the order of ~0.3 eV with respect to the same molecular orbital of the rhodium complexes. The calculations with different atomic basis functions (Ir and Rh and various oxidation states) showed that the same approximate description is obtained in each case. Quantitative comparison of the small changes is questionable due to the approximate nature of the wave functions and the neglect of relativistic and other effects.

Results and Discussion

Background Description of the Electronic Structure. With the metals located in a square-planar environment and the coordinate system shown in Figure 1, the d_{xy} orbital of each iridium center accepts ligand σ electron donation from the two cis-coordinated carbonyls and the two σ-donating nitrogens of the pyrazolyls. The other predominantly metal d orbitals are fully occupied for these d^8 metals, and the general order of these levels is the usual square-planar pattern, with adjustment as shown below for the actual geometry and ligands of this complex:

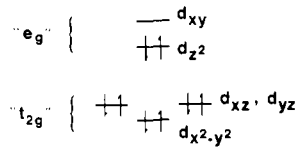

The $d_{x^2-y^2}$ orbital has some additional stabilization compared to that in the usual ligand field diagram because of π back-bonding to each of the cis carbonyls. Because of the manner in which the pyrazolyl ligands bridge the two metal centers, the square planes of each of the iridiums are tied together and the atomic d_{z^2} orbital of each metal is partially oriented toward the other. Increasing metal–metal interaction of the d_{z^2} orbitals along the axis produces greater destabilization due to filled–filled repulsion.

To help illustrate the electronic effects of methyl substitution on the pyrazolyls, photoelectron spectra of 1*H*-pyrazole and 1*H*-3,5-dimethylpyrazole are compared in Figure 2. The ionizations of 1*H*-pyrazole have been assigned previously.[18] A correlation diagram that uses the experimentally measured ionizations is shown in Figure 3. The outer valence π ionizations of a cyclopentadienyl ligand[19] are included to clarify the origin of the pyrazole π orbitals and the effects of methylation on the pyrazole π ionizations. The e_1'' set of cyclopentadienyl orbitals correlates with the 2a″ and 3a″ (C_s symmetry) orbitals of 1*H*-pyrazole. Each of these filled ring π orbitals possesses a single node perpendicular to the ring. The node in the pyrazole 3a″ molecular orbital lies close along the 3- and 5-carbons, allowing for little π overlap interaction with substituents on carbons 3 and 5. However, the node found in the 2a″ molecular orbital bisects the nitrogen–nitrogen bond and the carbon in the 4-position and allows for greater atomic p_π orbital contribution from carbons 3 and 5. Upon methylation of 1*H*-pyrazole in the 3- and 5-positions, all the ionizations shift to lower ionization energy. Table I gives the ionization energies and the shifts from 1*H*-pyrazole to 1*H*-3,5-dimethylpyrazole. The 2a″ ionization shifts to a slightly greater extent than 3a″, since the filled–filled interaction of the methyl e with the pyrazole π system is a greater effect for 2a″ than for 3a″.[19] It follows that the coordination of the methylated pyrazolyl ligand will further destabilize the metals to which it is bound either through increased direct σ donation from the less stable nitrogen lone pairs or through metal interaction with the π system of the pyrazolyl ligand.

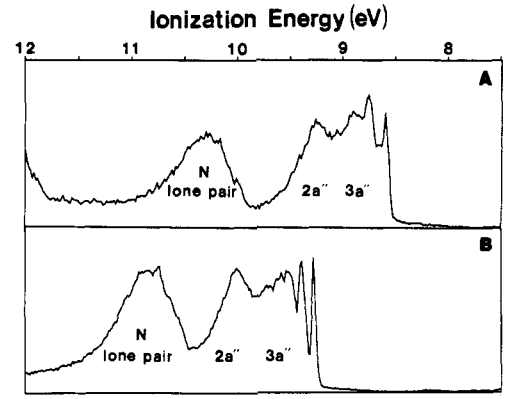

Figure 2. Photoelectron spectra (He I source) from 7.5 to 12 eV of (A) 1*H*-3,5-dimethylpyrazole and (B) 1*H*-pyrazole.

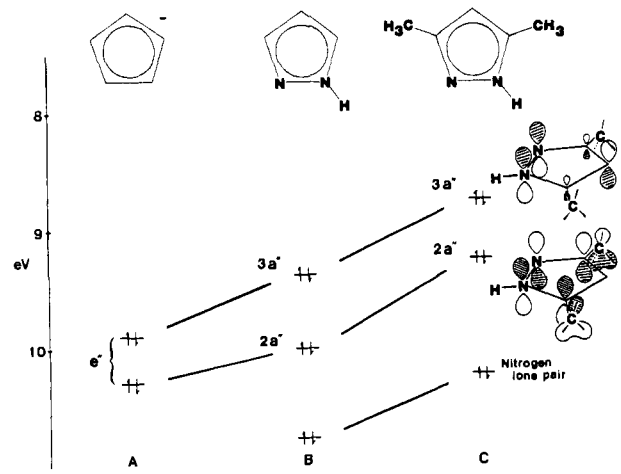

Figure 3. Correlation diagram of ring π and nitrogen lone-pair orbitals based on experimental ionizations of (A) cyclopentadienyl anion (from $(\eta^5\text{-}C_5H_5)Mn(CO)_3$[16]), (B) 1*H*-pyrazole, and (C) 1*H*-3,5-dimethylpyrazole.

Table I. Pyrazole Ionization Energies and Shifts with Methylation

peaks	IE, ±0.03 eV: 1*H*-pyrazole	IE, ±0.03 eV: 1*H*-3,5-dimethylpyrazole	shift, eV
3a″	9.38	8.75	0.63
2a″	10.01	9.26	0.75
N lone pair	10.78	10.23	0.55

Results of Calculations. Calculations on these iridium dimers yield three general classes of molecular orbitals. The highest occupied MO (HOMO) and the second highest occupied MO

(17) Clementi, E.; Roetti, C. *At. Data Nucl. Data Tables* **1974**, *14*, 177.
(18) Cradock, S.; Findlay, R. H.; Palmer, M. H. *Tetrahedron* **1973**, *29*, 2173.
(19) Calabro, D. C.; Hubbard, J. L.; Blevins, C. H., II; Campbell, A. C.; Lichtenberger, D. L. *J. Am. Chem. Soc.* **1981**, *103*, 6839.

Table II. Predominant[a] Percent Orbital Character in Ir Dimers

MO's		$5d_{z^2}$	$5d_{xy}$	$5d_{x^2-y^2}$	$5d_{xz}$	$5d_{yz}$	6s	6p	pz π 2a″	pz π 3a″	pz lp	CO π^*	CO 5σ	energy, eV
						[Ir(μ-pz)(CO)$_2$]$_2$, Ir–Ir Distance 3.51 Å								
$13b_1$	σ^*	79					18				2			9.36
$16a_1$	σ	78					19							9.67
$14a_2$	"t_{2g}"				77					8		10		10.63
$15a_1$				42		18				15		16		10.65
$11b_2$					78				7			10		10.91
$12b_1$				22		40			15			17		10.93
$14a_1$				20		56						15		11.09
$11b_1$				39		34			5			18		11.30
$13a_2$	pz π				7					82				13.32
$10b_2$					6				91					13.72
$13a_1$				9		3				70				13.92
$10b_1$				11		4			76					14.35
$9b_2$	pz lp		4					19			54		14	16.71
$9b_1$								20			56		11	17.29
$12a_1$								15			53		17	17.50
$12a_2$								16			44		23	17.72
						[Ir(μ-pz)(CO)$_2$]$_2$, Ir–Ir Distance 3.25 Å								
$13b_1$	σ^*	73					16				4			9.10
$16a_1$	σ	71		4			18							10.22
$15a_1$	"t_{2g}"	2		43		12				19		16		10.71
$14a_2$					77					8		12		10.92
$12b_1$				39		17			24			14		11.09
$11b_2$					80				5			12		11.18
$11b_1$				17		55						16		11.35
$14a_1$		3		11		65						12		11.49
$13a_2$	pz π				7					82				13.17
$10b_2$					4				93					13.57
$13a_1$				14		2				65				13.94
$10b_1$				16		2			70					14.37
$9b_2$	pz lp		4					20			53		13	16.95
$9b_1$		2						19			56		12	17.09
$12a_1$								15			55		14	17.46
$12a_2$								16			46		21	17.70
						[Ir(μ-3,5-Me$_2$pz)(CO)$_2$]$_2$, Ir–Ir Distance 3.25 Å								
$16b_1$	σ^*	74					16				4			8.91
$19a_1$	σ	72		3			18							10.07
$18a_1$	"t_{2g}"	2		44		11				20		16		10.60
$15b_1$				41		8			32			13		10.72
$17a_2$					78					6		12		10.80
$14b_2$					76				10			12		10.96
$14b_1$				10		63						14		11.20
$17a_1$		3		11		65						13		11.35
$13b_2$	pz π				8					87				12.89
$16a_2$					6				79					13.03
$16a_1$				13		2			64					13.75
$13b_1$				21		3				62				13.88
$12b_2$	pz lp		5					17			51		10	16.52
$12b_1$			3					17			53		9	17.66
$15a_1$								14			57		11	17.07
$15a_2$								15			48		17	17.34

[a] Any contributions from the other carbonyl and pyrazolyl framework MO's have not been included and can account for as much as ~20% of the total orbital character, especially for the pyrazolyl MO's.

(SHOMO) are predominantly metal d_{z^2} (71–79%), with some metal 6s (16–19%) character. These form the antibonding σ^* (HOMO) and bonding σ (SHOMO) combinations of the metal atomic d_{z^2} orbitals. The next six orbitals originate from the two metal "t_{2g}" sets. The calculated characters and energies of these orbitals are summarized in Table II. These "t_{2g}" orbitals are primarily metal in character but may contain anywhere from 5 to 32% pyrazolyl π character and 10–18% carbonyl π character. The remaining valence orbitals are the pyrazolyl π orbitals and the pyrazolyl nitrogen lone pairs, respectively.

Methylation of the pyrazolyl ligands causes an appreciable change in the geometry of the complex, in addition to the anticipated change in electron distribution. A significant feature of the change in geometry is that the metal–metal distance decreases from 3.51 to 3.25 Å with 3,5-methylation of the pyrazolyl ligand, and the angle between the iridium square planes produces greater overlap between the d_{z^2} orbitals. In order to help separate the electronic and geometric effects, calculations for the complex without methyl groups in the 3,5-positions were also carried out by using the geometry of the methylated complex. These overall results are illustrated in Figure 4. The calculations predict that the splitting between the antibonding σ^* and bonding σ combinations is sensitive to this geometry change. The calculated splitting at the long distance (pyrazolyl) is about 0.3 eV compared to the splitting at the shorter distance (3,5-pyrazolyl) of about 1.1 eV. This increased splitting of the σ^* and σ combinations with shorter metal–metal distance results in a net destabilization of the antibonding σ^* orbital of about 0.3 eV. There is also a slight increase in pyrazolyl π character in the metal orbitals (16% maximum at long metal–metal distances to 24% maximum at short metal–metal distances and without methyl substitution). All of these points are significant for understanding the valence ionizations.

When methyl groups are placed on the 3,5-positions of the bridging pyrazolyls, the calculations show an average destabilization of 0.4 eV of all the pyrazolyl molecular orbitals (see Table

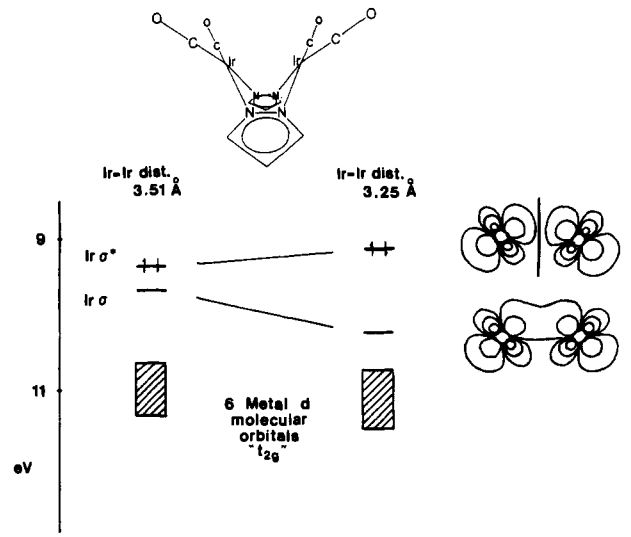

Figure 4. Fenske–Hall molecular orbital diagram of the metal-based orbitals of $[Ir(\mu\text{-pz})(CO)_2]_2$ in its normal geometry (3.51-Å Ir–Ir distance) and in the geometry of the 3,5-methylated analogue (3.25-Å Ir–Ir distance).

II) and an increased negative charge on the pyrazolyl nitrogens. The pyrazolyl, in turn, contributes greater π character in the metal "t_{2g}" set (16% maximum pyrazolyl π character at long metal–metal distances to 32% maximum pyrazolyl π character at short metal–metal distances). These metal "t_{2g}" orbitals are calculated to shift nearly as much (0.3 eV) as the ligand-based orbitals with methylation. The splitting predicted between the σ^* and σ orbitals upon decrease in metal–metal distance is not affected by the change in electron distribution with methyl group substitution. However, the σ^* and σ orbital energies are both destabilized (0.19 and 0.15 eV, respectively).

Although the calculations yield some valuable insights into the trends in electronic interactions in these systems and provide the groundwork for understanding the experimental information that follows, the absolute values that are calculated for energies and shifts should not be considered definitive without further information. Uncertainties are inherent in any calculational approach, and heavy atoms such as iridium are difficult for current theoretical methods. The splitting between the metal–metal σ and σ^* orbitals is calculated to be fairly small for $[Ir(\mu\text{-pz})(CO)_2]_2$ and sensitive to the precise geometry. Calculations using iridium atomic basis functions with oxidation states from 0 to +2 and using the range of known geometries give splittings from 0.24 to 1.42 eV. Relativistic effects are likely to be equally significant. It is clear that experimental information relating to these interactions is essential for understanding the behavior of these complexes.

Information from Ionization Characteristics. Photoelectron spectroscopy experimentally measures the gas-phase ionization energies and therefore gives a quantitative measure of the trends in energy splitting with geometry change and shift with pyrazolyl methylation. The spectra of $[Ir(\mu\text{-pz})(CO)_2]_2$, $[I(\mu\text{-3-Me-pz})(CO)_2]_2$, and $[Ir(\mu\text{-3,5-Me}_2\text{-pz})(CO)_2]_2$ from 7 to 12 eV are shown in Figure 5. The valence ionization features from 7 to 12 eV are very similar for each complex. The assignments of the valence ionizations below 12 eV binding energy are given in Table III. These assignments are based on correlations with the ionizations of free pyrazole[15] and other d^8 square-planar complexes.[20-22] The general ordering of the ionizations is the same as that calculated by the Fenske–Hall method. The ionizations above 9-eV binding energy are predominantly ligand-based. Bands C and D are derived from pyrazolyl nitrogen lone pairs (bonding and antibonding combinations), and bands A and B correlate with pyrazolyl π orbitals. The broad band M corresponds primarily to the metal electrons of "t_{2g}" parentage from the square-planar metal centers. Ionization band I represents the electrons derived from the predominantly metal d_{z^2} orbitals and completes the d^8 configuration of the metals.

The analysis of the lowest ionization energy band (band I) is particularly crucial to the interpretation of the behavior of these complexes. Close-up examinations of the leading ionizations are shown in Figure 6. The two highest occupied orbitals are expected to be the σ and σ^* combinations of the two iridium d_{z^2} orbitals. It is important to determine if the broad leading ioization band contains both the σ and σ^* ionizations, indicating that the interaction between the d_{z^2} orbitals on each iridium is of little consequence to the electronic structure, or if the leading ionization

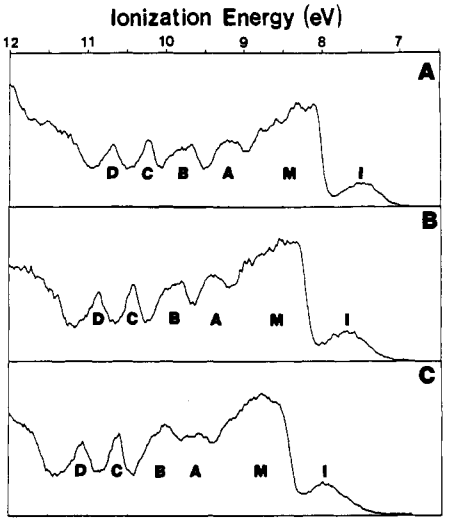

Figure 5. Photoelectron spectra (He I source) from 7 to 12 eV of (A) $[Ir(\mu\text{-3,5-Me}_2\text{-pz})(CO)_2]_2$, (B) $[Ir(\mu\text{-3-Me-pz})(CO)_2]_2$, and (C) $[Ir(\mu\text{-pz})(CO)_2]_2$.

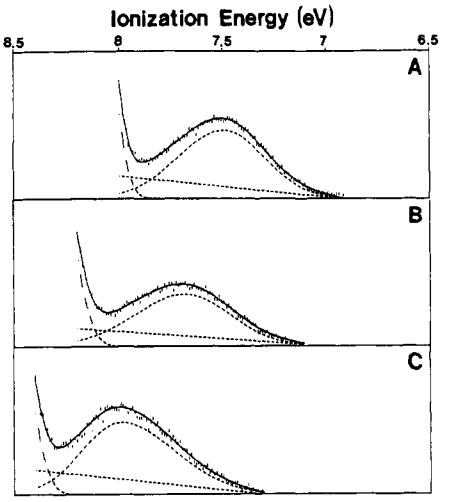

Figure 6. Close-up photoelectron spectra in the range of 7–8.5 eV of (A) $[Ir(\mu\text{-3,5-Me}_2\text{-pz})(CO)_2]_2$, (B) $[Ir(\mu\text{-3-Me-pz})(CO)_2]_2$, and (C) $[Ir(\mu\text{-pz})(CO)_2]_2$.

Table III. Vertical Ionization Energies

	IE, ±0.03 eV		
peak	$[Ir(\mu\text{-pz})(CO)_2]_2$	$[Ir(\mu\text{-3-Me-pz})(CO)_2]_2$	$[Ir(\mu\text{-3,5-Me}_2\text{-pz})(CO)_2]_2$
I	7.99	7.68	7.49
M[a]	8.54–9.25	8.31–8.93	8.09–8.65
A	9.63	9.46	9.25
B	10.05	9.83	9.69
C	10.61	10.41	10.22
D	11.06	10.86	10.69

[a] Range of the ionization envelope.

(20) Louwen, J. N.; Hengelmolen, R.; Grove, D. M.; Oskam, A.; DeKock, R. L. *Organometallics* **1984**, *3*, 908.
(21) Louwen, J. N.; Grove, D. M.; Ubbels, H. J. C.; Stufkens, D. J.; Oskam, A. *Z. Naturforsch., B: Anorg. Chem., Org. Chem.* **1983**, *28B*, 1657.
(22) Di Bella, S.; Fragala, I.; Granozzi, G. *Inorg. Chem.* **1986**, *25*, 3997.

Table IV. Relative Peak Areas Normalized to Relative Numbers of Electrons[a]

	metal		pz π		N	
	I	M	A	B	C	D
$[Ir(\mu\text{-pz})(CO)_2]_2$						
rel area	1.0	6.4	1.2	2.4	0.8	1.1
no. of electrons[b]	2.3	14.5	8			
$[Ir(\mu\text{-3-Me-pz})(CO)_2]_2$						
rel area	1.0	7.0	1.3	2.3	0.8	1.0
no. of electrons[b]	2.3	15.8	8			
$[Ir(\mu\text{-3,5-Me}_2\text{-pz})(CO)_2]_2$						
rel area	1.0	8.1	1.9	2.3	0.9	1.0
no. of electrons[b]	1.9	15.7	8			

	metal	Cp π
osmocene[c]		
rel area	1.0	1.355
no. of electrons	6	8

[a] The best fits of asymmetric Gaussian peaks were used to account for the area under each band. Overlap of the metal band M with the pyrazolyl π ionization contributes to an uncertainty of 15–20% in the estimation of the relative number of electrons under each band. [b] Relative to eight ligand-based π electrons. [c] Reference 24.

is a single ionization event attributable to σ^* only, indicating that the σ ionization is in the metal "t_{2g}" region M and is split well away from σ^*.

An indication of the number of ionizations in band I for each complex is provided by the area of the leading ionization band relative to those of the metal "t_{2g}" ionizations (band M) and the ligand-based ionizations (bands A–D). First, the relative area of the leading peak compared to that of two peaks (C and D) at higher ionization energy remains constant through the series of iridium compounds (the average area of band I relative to that of band D is 1.04 ± 0.06 and the area of band I relative to that of band C is 0.84 ± 0.04). This consistency in relative peak area indicates that the number of ionizations under the leading band is the same throughout the series. Second, the relative peak areas listed in Table IV show that the area ratio of band M to band I varies from a low of 6.3:1 for the pyrazolyl complex to a high of 8.3:1 for the 3,5-dimethylpyrazolyl complex. This is in good agreement with the approximate 7:1 ratio expected if band I represents just the σ^* ionization and is more than a factor of 2 away from the 3:1 ratio expected if both the σ and σ^* ionizations were contained in band I.

Assignments based only on relative cross sections of metal ionizations should never be considered definitive. The conclusion that the initial ionization represents the σ^* ionization alone is strengthened by other measurements and theoretical calculations of the relative cross sections of the metal-based ionizations and ligand-based ionizations. The photoelectron spectrum of osmocene provides a good standard for experimentally comparing the ionization cross sections of a third-row metal with those of a five-membered organic ring π system. The ionization assignments for osmocene[23] and the number of electrons represented by each ionization in the region of 6–12 eV are very clear. The vibrational fine structure and spin–orbit splitting observed for the ionization bands of osmocene provide experimental measures of the relative ligand and metal characters of the ionizations.[24] The large separation of the ionization bands allows for an accurate determination of the relative band area for the ring π ionizations in comparison to that of the third-row-metal ionizations. For comparison of the osmocene cross sections to the iridium complex ionizations, theoretical calculations indicate that the absolute cross sections of the neighboring third-row metals osmium and iridium differ by 5–10%.[25] Similar small differences will arise from comparison of primarily ligand π ionizations of the cyclopentadienyl group with the π ionizations of the pyrazolyl group

Table V. Half-Widths of the Leading Ionization Bands (eV)

compd	W_h[a]	W_l[a]	total width
$[Ir(\mu\text{-pz})(CO)_2]_2$	0.44	0.61	0.52
$[Ir(\mu\text{-3-Me-pz})(CO)_2]_2$	0.58	0.50	0.54
$[Ir(\mu\text{-3,5-Me}_2\text{-pz})(CO)_2]_2$	0.52	0.46	0.49

[a] See Experimental Section for definition of symbols.

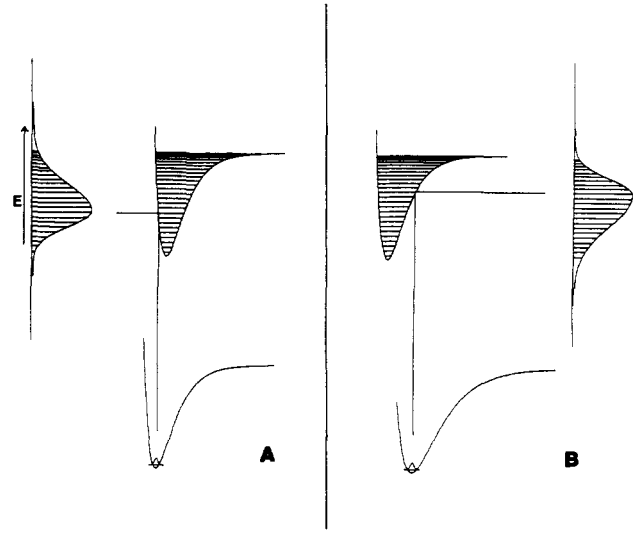

Figure 7. Representative ionization band shapes: (A) ionization from a bonding orbital; (B) ionization from an antibonding orbital.

and the different delocalizations in the osmocene and iridium complexes. Thus, the confidence limits in this cross-section correlation are more than adequate for determining whether one or two ionization states contribute to the initial ionization band of these iridium dimers.

The relative areas for the ring ligand π and metal ionizations of the osmocene and iridium complexes are shown in Table IV. The ratio of the cyclopentadienyl π ionization area (representing eight ring π electrons) to the total metal band area (which represents six metal electrons) in osmocene is compared with the combined pyrazolyl ring π area (again representing eight ring π electrons) and the iridium-based ionizations in bands I and M. These relative areas are used to determine the number of electrons in the metal-based ionizations that are reported in Table IV. It is found that the leading ionization represents two electrons corresponding to the σ^* ionization only. There is sufficient area under band M to account for the σ ionization as well as the "t_{2g}" ionizations.

The band shape of the leading ionization of $[Ir(\mu\text{-pz})(CO)_2]_2$ is also very significant. It is very broad and is observed to have a pronounced asymmetric band shape that does not clearly reveal separate ionization features. The total bandwidth actually narrows slightly with methylation, which is counter to what one would expect if both σ and σ^* were under this envelope and the metal–metal interaction increased with methylation as calculated. The fit of a single asymmetric Gaussian profile to the leading band of $[Ir(\mu\text{-pz})(CO)_2]_2$ shows most clearly that the low binding energy half-width of the band is greater than the high binding energy half-width (see Table V). This skew of an ionization to low binding energy is quite rare. For ionizations that occur from a bonding or nonbonding orbital to a single ion state, the half-width for the low ionization energy side of the band is always observed to be less than the half-width for the high ionization energy side of the band.[26] This is because the slope of the positive ion potential well allows ionization to more vibrational quanta above the vertical ionization than below the vertical ionization (see Figure 7). An exception can occur when an ionization from an antibonding orbital causes a decrease in equilibrium bond distance in the positive ion. In this case, the slope and dissociation limit on this

(23) Evans, S.; Green, M. L. H.; Jewitt, B.; Orchard, A. F.; Pygall, C. F. *J. Chem. Soc., Faraday Trans. 2* **1972**, *68*, 1847.
(24) Copenhaver, A. S.; Lichtenberger, D. L., submitted for publication.
(25) Yeh, J. J.; Lindau, I. *At. Data Nucl. Data Tables* **1985**, *32*, 7.
(26) Lichtenberger, D. L. *Diss. Abstr. Int., B* **1975**, *35*, 4856.

Table VI. Shifts in Ionizations with Methyl Substitution of the Pyrazolyls from IE's of $[Ir(\mu\text{-pz})(CO)_2]_2$

	total shift, ±0.04 eV	
peaks	$[Ir(\mu\text{-3-Me-pz})(CO)_2]_2$	$[Ir(\mu\text{-3,5-Me}_2\text{-pz})(CO)_2]_2$
I	0.31	0.50
M[a]	0.23	0.45
A	0.17	0.38
B	0.22	0.32
C	0.20	0.38
D	0.20	0.37

[a] Shifts in energy of band M are measured from the low-ionization-energy leading edge.

side of the potential well of the positive ion limit the number of vibrational quanta accessible above the vertical ionization, allowing the possibility of more ionizations to vibrational quanta below the vertical ionization than above. Thus, the anomalous shape of the band in this complex indicates that this ionization is from the antibonding metal–metal σ^* orbital and that upon ionization the equilibrium bond distance of the positive ion has decreased. This is consistent with a net zero bond order between the metals in the neutral molecule and a net $^1/_2$ bond order between the metals in the ground state of the positive ion, with significant interaction between the metals.

Ionization Shifts with Pyrazolyl Methylation. The pronounced shifts of the bands to lower ionization energy upon methylation of the pyrazolyl ligand are summarized in Table VI. The shifts are primarily due to the destabilization of the pyrazolyl π and nitrogen lone-pair donor orbitals upon addition of methyl groups to the pyrazolyl ligand and the additional donation of electron density from these orbitals to the iridium atoms of the molecule. The shifts with pyrazolyl methylation are additive within the uncertainty of the data. That is, the shift for pyrazolyl methyl groups in the 3- and 5-positions is approximately twice the shift for a methyl group in the 3-position. Interestingly, the band that shifts to the greatest extent with methylation is not ligand-based but is instead the leading ionization, band I. The metal "t_{2g}" envelope has the next most predominant shift, and the pyrazole π and pyrazole nitrogen lone pairs tend to shift the least.

The major portion of the shift to lower ionization energy exhibited by the leading band is due to the inductive effect of the methyl-substituted pyrazolyl on the metal. However, the inductive shift of the leading ionization band will not be more than the shift of the pyrazolyl π and lone-pair ionizations with methylation. The additional shift of the leading ionization band is likely due to an increased splitting between the Ir_2 σ and σ^* orbitals with the decrease in metal–metal distance found for the methylated complex. This produces additional destabilization of σ^* and a lower binding energy ionization.

Shifting in the metal "t_{2g}" ionizations follows from the interaction of these levels with the filled π system of the pyrazolyls. Calculations predict a substantial (6–32%) percent of pyrazolyl π interaction with the metal "t_{2g}" orbitals, which facilitates the delocalization of methyl group electron density to the metal centers. The extent of this mixing increases with methylation. As implied by the decrease in the range of ionization energies in the metal region M (see Table III), a few of the metal ionizations have been shifted more than other metal ionizations. The range decreases from 0.71 to 0.62 eV upon addition of one methyl group to each pyrazolyl and from 0.62 to 0.56 eV with the addition of the last methyl group set, for a total narrowing of the metal "t_{2g}" band region of 0.15 eV. As reflected by the shift diagram of pyrazole π orbitals, metal orbitals with greater pyrazolyl π (2a″) orbital character should shift to a greater extent. The large metal band shifts emphasize the fact that the metals are significantly influenced by the substitution of methyl groups on the pyrazolyls.

Fenske–Hall calculations predict that a decrease in the metal–metal distance will increase the splitting between the σ and σ^* molecular orbitals by 0.8 eV or more. The calculated increase in splitting between σ and σ^* is not observed directly in the photoelectron spectra of this series of iridium dimers, since the σ ionization is buried under the "t_{2g}" ionization band. However, if we expect the shift due only to methyl substitution on the leading ionization to be generally the same as the shift found for the metal "t_{2g}" region, then the added shift found in the leading ionization is due to the increased splitting expected between the σ and σ^* ionizations upon decrease in metal–metal distance. This increased shift due to metal–metal interaction is estimated to be a minimum of 0.05 eV. Thus, the major portion of the ~0.5-eV shift to lower energy of the leading ionization band is due to inductive effects of methyl substitution on the pyrazolyl ligands. The Fenske–Hall calculations apparently overestimate the destabilization due to the decrease in Ir–Ir distance (0.8 eV) and underestimate the destabilization due to the inductive effects of the methyl group substitution (0.2 eV). Shifting of the σ^* ionization caused by the decrease in metal–metal distance appears to be a secondary contribution.

Table VII. Metal–Metal Distances and Chemistry for Related Ir Dimers

	M–M dist, Å	reacn
$[Ir(\mu\text{-3,5-Me}_2\text{-pz})(COD)]_2$[a]		oxidative addition
$[Ir(\mu\text{-pz})(COD)]_2$	3.216	oxidative addition
$[Ir(\mu\text{-3,5-Me}_2\text{-pz})(CO)_2]_2$	3.245	hydrogenation catalyst
$[Ir(\mu\text{-3-Me-pz})(CO)_2]_2$		no catalytic activity
$[Ir(\mu\text{-pz})(CO)_2]_2$	3.502	no catalytic activity
$[Ir(\mu\text{-3,5-(CF}_3)_2\text{-pz})(COD)]_2$	3.073	inert

[a] COD = 1,5-cyclooctadiene.

Reactivity Trends and Ionization Energies. Table VII lists six representative iridium dimer complexes that exhibit a variety of metal–metal distances and reactivities. Some of these complexes have been known to undergo oxidative addition, while others are inert. It was surmised that the shorter metal–metal distances generally lead to higher reactivity.[2] However, the compound with the shortest metal–metal distance, $[Ir(\mu\text{-3,5-(CF}_3)_2\text{-pz})(COD)]_2$, was found to be inert. It was proposed that the lack of reactivity found for $[Ir(\mu\text{-3,5-(CF}_3)_2\text{-pz})(COD)]_2$ was due to steric blockage of reactive sites on the metals by the trifluoromethylated pyrazolyl groups and that otherwise the short metal–metal distance would encourage reactivity. However, $[Ir(\mu\text{-3,5-Me}_2\text{-pz})(COD)]_2$ is at least as sterically hindered and this complex reacts to form oxidative-addition products. This observation leads us to believe that electronic interactions are of primary importance in determining the Ir_2 chemistry.

The photoelectron spectroscopy results show that the frontier metal orbitals are extremely sensitive to substitution on the pyrazolyls. While steric considerations must be taken into account, the electronic influence of substitution of the pyrazolyl groups strongly affects the frontier-orbital-controlled reaction chemistry of these iridium dimers. The ability of methyl substitution of the pyrazolyls to reduce the ionization energies allows for easier oxidation and greater reactivity with the destabilized HOMO. The replacement of the carbonyls by cyclooctadienyls will also facilitate the oxidative-addition chemistry because of the loss of π-electron-withdrawing ability of the ligands. The strong electron-withdrawing power of the trifluoromethyl group[27,28] in $[Ir(\mu\text{-3,5-(CF}_3)_2\text{-pz})(COD)]_2$ has the opposite effect, stabilizing the HOMO (σ^*) and making oxidation and related reactions more difficult.

Acknowledgment. D.L.L. acknowledges support by the U.S. Department of Energy (Division of Chemical Sciences, Office of Basic Energy Sciences, Office of Energy Research, Contract No. DE-AC02-80ER10746), the National Science Foundation (Grant No. CHE8519560), and the Materials Characterization Program, Department of Chemistry, University of Arizona. Research at the California Institute of Technology was supported by NSF Grant No. CHE8419828.

(27) Gassman, P. G.; Winter, C. H. *J. Am. Chem. Soc.* **1986**, *108*, 4228.
(28) Paddon-Row, M. N.; Santiaso, C.; Houk, K. N. *J. Am. Chem. Soc.* **1980**, *102*, 6561.